The Impact of Feeder Link Interference in Multiple Gateway Multibeam Satellite Systems

Vahid Joroughi and Carlos Mosquera
Signal Theory and Communications Department, University of Vigo, 36310-Vigo, Spain.
Emails: vahid.joroughi@gts.uvigo.es, mosquera@gts.uvigo.es

***Abstract*—High throughput satellites rely on the reuse of spectrum across different beams. To this end, beams are synthesized by complex array fed reflectors. Multiuser techniques such as precoding can make viable an aggressive reuse of the spectrum, even to the point of facilitating the path towards full frequency reuse deployments. This entails a high demand on the feeder link, which needs to be provisioned by multiple gateways in order to accommodate all the throughput. As a consequence, spectrum needs to be also reused by the different gateway-to-satellite links, potentially causing inter-feeder link interference in addition to the user link multiple beam interference. This paper addresses jointly the interference in both user and feeder links by proposing two novel precoding techniques. An analysis is provided to account for the additional degradation coming from the co-channel interference in the feeder link.**

***Index Terms*—Multibeam satellite systems, multi-gateway transmission, Inter-feeder links interference, MIMO precoding.**

I. Introduction

The use of multibeam broadband satellite systems have increased during the last few years, in an effort to keep up with the demand for higher throughput. A large number of beams is deployed on the coverage area so spectrum can be better exploited [1].

In this context, full frequency reuse pattern among beams is a promising scheme in order to increase available bandwidth resources. However, multibeam interference becomes the bottleneck of the communication, asking for interference mitigation techniques. Different studies have been made in the last years to apply precoding and multiuser detection in the forward and return link, respectively [2, 3].

On the other hand, as the number of beams increases, the ground and space units need to exchange higher volumes of data over the feeder link coming from all the feed signals on the satellite antenna. If the number of feeds is higher than the number of antennas, some on-board beamforming can be applied to reduce the number of signals to exchange with the ground, as shown in [4] and [9]. Even though this beamforming takes place on-board the satellite, the potential savings in throughput requirement for the feeder link are limited, and some other alternatives are needed. Another proposed solution would be to move feeder links into the Q/V bands, but this requires expensive site diversity to tackle outages due to atmospheric effects [5]. In this regard, multiple gateways that reuse the feeder link resources to distribute the communication capacity can be the preferred solution, by means of very directive antennas [6, 7]. Some additional benefits of a multiple gateway architecture include:

- Lower signal processing complexity, since each gateway handles a smaller number of beams.
- Increased reliability. In case of gateway failure, traffic can be rerouted through other gateways to avoid service outage.
- Backhauling cost reduction. Satellite service providers such as TV operators or Internet providers find valuable a set of gateways which are geographically distributed, so they can use that closer to their premises.

However, even with highly directive antennas the feeder links are partially interfering when each feeder link reuses the same frequency resources [6], in what is referred to as inter-feeder link interference. Therefore, the transparent feeder link assumption might not be valid anymore in contrast to the usual assumption in previous works [7], and careful evaluation is needed.

To cope with the increased level of interference in both feeder and user links, this work studies the forward link of a multiple gateway multibeam satellite system architecture where each gateway handles a set of beams. In contrast to previous works, we show that the impact of inter-feeder link interference changes the nature of the problem and can lead to a significant degradation of the average output Signal to Interference and Noise Ratio (SINR) on the coverage area. In consequence, we design especially tailored Multiple Zero Forcing (M-ZF) and Multiple Minimum Mean Square Error (M-MMSE) precoding techniques to account for both user link and feeder link interference, and with each gateway computing part of the full precoding matrix.

The paper is organized as follows. Section II presents an overview of the system model. The precoding techniques are presented in Section III. Section IV contains a summary of the simulation numerical results, with the conclusions provided in Section V.

The parameters relative to the architecture considered in this work were provided by the European Space Agency (ESA) in the framework of a study on next generation multibeam satellite systems.

Notation: Throughout this paper, the following notation will

This work was partially funded by the Spanish Ministry of Economy and Competitiveness and the European Regional Development Fund (ERDF) under project COMPASS (TEC2013-47020-C2-1-R), by the Galician Regional Government and ERDF under projects "Consolidation of Research Units" (GRC2013/009), REdTEIC (R2014/037) and AtlantTIC.

be adopted. Boldface uppercase letters denote matrices and boldface lowercase letters refer to column vectors. $(.)^H$ and $(.)^T$ denote Hermitian transpose and transpose matrices, respectively. $\mathbf{I}_N$ builds the $N \times N$ identity matrix. $[\mathbf{A}]^{i,i}$ and $[\mathbf{A}]^{i,j}$ with $i \neq j$ represent the block diagonal and off-diagonal submatrices of $\mathbf{A}$, respectively. Boldface $\mathbf{0}$ refers to an all-zero matrix. $\mathbf{A}_{ij}$ represents the (ith, jth) element of matrix $\mathbf{A}$ and $(\mathbf{A})_{K\times K}$ denotes a submatrix of $\mathbf{A}$ of size $K \times K$. $diag$ represents a diagonal matrix. Finally, $\mathrm{E}\{.\}$ and $||.||$ refer to the expected value operator and the Frobenius norm, respectively.

II. System Description

Consider the forward link of a multiple gateway multi-beam satellite communication system, where a single geosynchronous satellite with multibeam coverage provides broadband services to a large set of users. To this end, the satellite is equipped with an array fed reflector antenna, whose number of elements/feeds is denoted by N. The number of beams is denoted by K with

$$K \leq N, \tag{1}$$

and the users are assumed to be uniformly distributed within the beams. By employing a Time Division Multiplexed (TDM) scheme, at each time instant a total of K single antenna users, one per beam, is simultaneously served by a satellite relaying the data to Earth through a set of F gateways. In this context, each gateway serves a set of adjacent beams, and the corresponding routing between feeder links and antenna feeds is performed on the satellite. Even though the feeder link antennas are highly directive, a complete isolation between the different feeder links may not be realistic, giving rise to some interference on top of the existing among the beams. The feeder link is also affected by the atmospheric fading caused by rain attenuation, and some theoretical and experimental results are already available [5]-[6]. However, to the authors' knowledge no previous contributions exist on the inter-feeder link interference problem for multiple gateway settings, and this will be the focus of this work. Additional simulation work would be needed to quantify the impact of the feeder links fading.

In such scenario, the signals at the terminals can be modeled as

$$\mathbf{y} = \mathbf{H}_u \mathbf{H}_f \mathbf{x} + \mathbf{n} \tag{2}$$

where $\mathbf{y}$ is a $K \times 1$ vector containing the symbols received by K users, one per beam, at a given time instant. $N \times 1$ vector $\mathbf{x}$ denotes the stack of the transmitted signals at all feeds. The $K \times 1$ vector $\mathbf{n}$ contains the stack of zero mean and unit variance Additive White Gaussian Noise (AWGN) such that $\mathrm{E}\{\mathbf{n}\mathbf{n}^H\} = \mathbf{I}_K$. The matrix $\mathbf{H}_f$ of size $N \times N$ models the inter-feeder links interference for a given frequency reuse pattern. Let N_m denote the number of signal streams which needs to be transmitted through the feeder link from the m-th gateway to the satellite. Typically, those streams are transmitted in a frequency multiplexed fashion in the feeder link, such that the required bandwidth is directly proportional to N_m. Note that throughout this paper we consider an identical number of signal streams at the feeder link of each gateway so that

$$N_t \triangleq N_1 = ... = N_m = ... = N_F \tag{3}$$

where $N_{(.)}$ denotes the number feeder link resources at each gateway and N_t represents the equal number of feeder link signal streams at any gateway. Then, matrix $\mathbf{H}_f$ can be

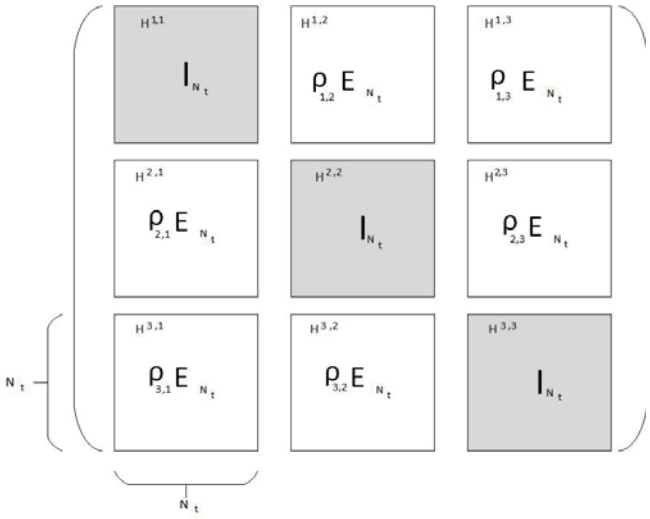

Fig. 1: The feeder link channel matrix decomposition for three gateways where each gateway generates an individual feeder link. Each block is a $N_t \times N_t$ submatrix of $\mathbf{H}_f$.

described by a set of submatrices $[\mathbf{H}_f]^{i,j}$ for $i = 1, \ldots, F$ and $j = 1, \ldots, F$. These submatrices, with dimension $N_t \times N_t$, model the inter-feeder link interference, so that each entry of $[\mathbf{H}_f]^{i,j}$, when $i \neq j$, quantifies the interference power level between the i-th and the j-th gateway. The amount of interference will be parameterized as follows:

$$[\mathbf{H}_f]^{i,i} = \mathbf{I}_{N_t}, \tag{4}$$

$$[\mathbf{H}_f]^{i,j} = \rho_{i,j}\mathbf{E}_{N_t} \quad i \neq j, \tag{5}$$

for $i = 1, \ldots, F$ and where $\mathbf{E}_{N_t}$ is a $N_t \times N_t$ matrix whose entries are equal to one. Moreover, $\rho_{i,j}$ is a parameter that models the overall interference gain level between i-th and j-th gateway feeder links. The larger ρ the larger feeder link interference is considered. For the sake of clarity, Figure 1 shows the decomposition of $\mathbf{H}_f$ for three gateways.

The user link channel $\mathbf{H}_u$ can be decomposed as follows:

$$\mathbf{H}_u = \mathbf{D}\mathbf{W} \tag{6}$$

where:

- $\mathbf{D}$ is assumed to be a $K \times K$ diagonal matrix which takes into account the atmospheric fading in the user link such that

$$\mathbf{D} = \mathrm{diag}\left(\frac{1}{\sqrt{A_1}}, ..., \frac{1}{\sqrt{A_K}}\right) \tag{7}$$

where A_k denotes the rain attenuation affecting the transmission to user k.

- $\mathbf{W}$ is a $K \times N$ matrix which models the feed radiation patterns, the path loss, the receive antenna gain and the noise power. The (k,n)-th entry of $\mathbf{W}$ is modeled as

$$w_{kn} = \frac{W_R \; g_{kn}}{4\pi \frac{d_k}{\lambda}\sqrt{k_B T_R B_W}} \tag{8}$$

where W_R^2 denotes the user receive antennas power gain. g_{kn} is referring to the gain (in power) from feed n to the k-th user, such that the respective feed transmit gain is $10\log_{10}(|w_{kn}|^2)$ if expressed in dBi. Finally, d_k is the distance between the k-th user and the satellite, λ the carrier wavelength, k_B the Boltzmann constant, T_R the receiver noise temperature, B_W the carrier bandwidth.

The reader can refer to [9] for a more detailed description of the user link channel model.

We will assume that every gateway can acquire perfect Channel State Information (CSI) about all gateways to user terminals, and that full frequency reuse is employed for both user beams and feeder links. Interference mitigation schemes have been proposed to reduce the impact of the high interference on the communication due to the aggressive frequency reuse. Due to their limited complexity, we will focus on linear schemes, in particular ZF and MMSE [10], to design the $N \times K$ precoding matrix $\mathbf{T}$ which is used to synthesize $\mathbf{x}$ in (2):

$$\mathbf{x} = \mathbf{T}\mathbf{s} \tag{9}$$

where $\mathbf{s}$ is the transmit symbol vector such that the k-th entry of $\mathbf{s}$ is the constellation symbol destined to the k-th user with

$$\mathrm{E}\{\mathbf{s}\mathbf{s}^H\} = \mathbf{I}_K. \tag{10}$$

The matrix $\mathbf{T}$ is obtained for both ZF and MMSE cases as

$$\mathbf{T}_{\text{ZF}} = \sqrt{\alpha}\mathbf{H}^H\left(\mathbf{H}\mathbf{H}^H\right)^{-1} \tag{11}$$

$$\mathbf{T}_{\text{MMSE}} = \sqrt{\alpha}\mathbf{H}^H\left(\mathbf{H}\mathbf{H}^H + \mathbf{I}_N\right)^{-1} \tag{12}$$

where

$$\mathbf{H} \triangleq \mathbf{H}_u\mathbf{H}_f. \tag{13}$$

The parameter α is such that the total power constraint P is met, that is,

$$\mathrm{E}\{||\mathbf{H_f x}||^2\} = \text{trace}(\mathbf{H}_f\mathbf{T}\mathbf{T}^H\mathbf{H}_f^H) \leq P. \tag{14}$$

We assume that the transmitted power is managed by a Traveling Wave Tube Amplifiers (TWTAs) architecture, with flexible allocation of power to beams [8] and the computationally complex power allocation schemes are out of the scope of this paper.

Next section describes how precoding matrices in (11) and (12) should be obtained in a multiple gateway architecture.

III. Precoding design

This section shows the steps to design M-ZF and M-MMSE precoders which have to cope simultaneously with interference in both user and feeder links in a multiple gateway structure. Each gateway handles a reduced number of beams, and the following assumptions will be made to simplify the derivations:

- The number of on-board feed signals and feeder link streams, denoted by $N_{\text{on-board feed}}$ and $N_{\text{feeder link}}$, respectively, are identical. $N_{\text{feeder link}}$ determines the number of total streams which need to be transmitted in the feeder link from F gateways. The satellite is equipped with F feeder link receivers and the feeder link streams are demultiplexed and routed with an identical number of on-board feed signals, i.e. $N_{\text{on-board feed}}$, at the array fed reflector.
- Each gateway serves a set of adjacent users and beams which we will refer to as a *cluster* of beams. In other words, a cluster consists of a set of adjacent beams which are served by a single individual gateway. Therefore, there is *an equal number of gateway and clusters*. Additionally:
  - All clusters serve an identical number of beams. For instance, since the number of served beams in m-th cluster is denoted by K_m, for a total number of F clusters we have that

$$K_t \triangleq K_1 = ... = K_m = ... = K_F \tag{15}$$

    Note that an identical number of signal streams at the feeder link of each gateway/cluster is considered (see Equation (3)).
  - In a given time instant (e.g, at TDMA scheme), only a single user per-beam is served.
- $\bar{K}_m$ denotes the number of users served by other clusters different from m-th cluster, so that

$$\bar{K}_t \triangleq \bar{K}_1 = ... = \bar{K}_m = ... = \bar{K}_F \tag{16}$$

  and $K_t + \bar{K}_t = K$, with $K_t < \bar{K}_t$.
- Vector $\mathbf{s}_m$ denotes the symbols addressed to the users served by the m-th gateway, with all symbols grouped in vector $\mathbf{s}$:

$$\mathbf{s} = \left(\mathbf{s}_1^H, ..., \mathbf{s}_m^H, ..., \mathbf{s}_F^H\right)^H. \tag{17}$$

  Gateways do not exchange symbols, so that the m-th gateway has just access to the symbols in $\mathbf{s}_m$.
- $\bar{N}_m$ denotes the number of feeder links resources which need to be transmitted from adjacent feeder links of m-th gateway to the satellite (i.e. white submatrixes in Fig. 1). For F gateways it is assumed that

$$\bar{N}_t = \bar{N}_1 = ... = \bar{N}_m = ... = \bar{N}_F \tag{18}$$

  where $N_t + \bar{N}_t = N$ and

$$N_t < \bar{N}_t \tag{19}$$

In the multiple gateway architecture under study, precoding is designed to mitigate intra-cluster, inter-cluster and inter-feeder

links interference. Considering m-th cluster, the intra-cluster interference refers to the interference received by each beam located into the m-th cluster from other users/beams in the same cluster (i.e. m-th cluster). In addition, the interference generated by a beam belonging to the m-th cluster on beams in other clusters is known as inter-cluster interference. The inter-feeder link interference at m-th gateway refers to the level of interference leaked from the feeder link of adjacent gateways. In this context, considering the decomposition of matrix $\mathbf{H}$ in (13), $\mathbf{H}_u^m = (\mathbf{H}_u)_{K_m \times N_m}$ and $\mathbf{H}_f^m = (\mathbf{H}_f)_{N_m \times N_m}$ with $m = 1, ..., F$ are submatrices obtained by selecting $K_m \times N_m$ and $N_m \times N_m$ of $\mathbf{H}_u$ and $\mathbf{H}_f$ and represent the corresponding channel of the beams located in m-th cluster and the the feeder link signals required to employ in order to transmit signal from m-th gateway to the satellite, respectively. On the other side, $\bar{\mathbf{H}}_u^m = (\bar{\mathbf{H}}_u)_{\bar{K}_m \times N_m}$ and $\bar{\mathbf{H}}_f^m = (\bar{\mathbf{H}}_f)_{\bar{N}_m \times N_m}$ denote the $\bar{K}_m \times N_m$ and $\bar{N}_m \times N_m$ submatrices obtained of $\mathbf{H}_u$ and $\mathbf{H}_f$ and indicate the interference received from beams located in m-th cluster on adjacent clusters/beams and inter feeder link interference imposed from m-th gateway to adjacent gateways, respectively. Besides, $\mathbf{T}_m$ of size $N_m \times K_m$ refers to the precoder in m-th gateway. We assume gateways are connected together by optical links so that the m-th gateway has access to

- $\mathbf{H}_u^m$ and $\mathbf{H}_f^m$ through m-th cluster
- $\bar{\mathbf{H}}_u^m$ and $\bar{\mathbf{H}}_f^m$ via adjacent gateways.

Note that the same approach can be extended for the rest of gateways and clusters. Then, the signal model in (2) for a total number of F gateways and clusters can be written as

$$\begin{pmatrix} \mathbf{y}_1 \\ \hline \vdots \\ \hline \mathbf{y}_m \\ \hline \vdots \\ \hline \mathbf{y}_F \end{pmatrix} = \mathbf{H}\ \text{diag}\left(\mathbf{T}_1\ ...\ \mathbf{T}_m ... \mathbf{T}_F\right) \begin{pmatrix} \mathbf{s}_1 \\ \hline \vdots \\ \hline \mathbf{s}_m \\ \hline \vdots \\ \hline \mathbf{s}_F \end{pmatrix} + \begin{pmatrix} \mathbf{n}_1 \\ \hline \vdots \\ \hline \mathbf{n}_m \\ \hline \vdots \\ \hline \mathbf{n}_F \end{pmatrix}. \tag{20}$$

For the design of the precoder matrices, $\mathbf{H}$ in (20) is decomposed as expressed in the Remark 1, where each gateway serves K_t beams via N_t feeds. As illustration, Figure 2 depicts the block diagram and channel decomposition for three gateways and clusters. For design purposes, the precoding matrices in (20) are conveniently decomposed, for $m = 1, ..., F$, as

$$\mathbf{T}_m = \mathbf{T}_{a_m} \mathbf{T}_{b_m} \tag{21}$$

where $\mathbf{T}_{a_m}$ is designed to mitigate the inter-feeder link interference at the m-th gateway, and $\mathbf{T}_{b_m}$ targets the inter- and intra-cluster interference at the m-th gateway.

Remark 1: Decomposition of matrix $\mathbf{H}$ for F gateways.

Matrix $\mathbf{H}$
Data: $N_t = N_1 = ... = N_m = ... = N_F$
Data: $\bar{N}_t = \bar{N}_1 = ... = \bar{N}_m = ... = \bar{N}_F$
Data: $K_t = K_1 = ... = K_m = ... = K_F$
Data: $\bar{K}_t = \bar{K}_1 = ... = \bar{K}_m = ... = \bar{K}_F$
Result: Decomposition of $\mathbf{H}_u$ and $\mathbf{H}_f$
initialization $\mathbf{H}_f$;
for *m=1, ... ,F* **do**
  Calculate
    $[\mathbf{H}_f^m]^{m,m} = \mathbf{I}_{N_t}$
    $[\mathbf{H}_f^m]^{m,j} = \rho_{m,j}\mathbf{E}_{N_t} \qquad m \neq j$
Then;
for *m=2, ... ,F* **do**
  Cluster/gateway 1:
  $\mathbf{H}_u^1 = \left(\mathbf{H}_u\right)_{K_t \times N_t}$
  $\mathbf{H}_f^1 = \left(\mathbf{H}_f\right)_{\bar{N}_t \times N_t} = \mathbf{I}_{N_t}$
  $\bar{\mathbf{H}}_u^1 = \left(\mathbf{H}_u\right)_{\bar{K}_t \times N_t}$
  $\bar{\mathbf{H}}_f^1 = \left(\mathbf{H}_f\right)_{\bar{N}_t \times N_t}$
  Cluster/gateway 2 to F:
  $\mathbf{H}_u^m = \left(\mathbf{H}_u\right)_{K_m \times N_m}$
  $K_m \triangleq (m-1)(K_t+1) : mK_t$
  $N_m \triangleq (m-1)(N_t+1) : mN_t$
  $\mathbf{H}_f^m = \left(\mathbf{H}_f\right)_{N_m \times N_m} = \mathbf{I}_{N_t}$
  where;

$$\bar{\mathbf{H}}_u^m = \begin{pmatrix} \bar{\mathbf{H}}_u^{m,1} \\ \bar{\mathbf{H}}_u^{m,2} \end{pmatrix}_{\bar{K}_m \times N_m}$$

$$\bar{\mathbf{H}}_f^m = \begin{pmatrix} \bar{\mathbf{H}}_f^{m,1} \\ \bar{\mathbf{H}}_f^{m,2} \end{pmatrix}_{\bar{N}_m \times N_m}$$

  so that;
  $\bar{\mathbf{H}}_u^{m,1} = \left(\mathbf{H}_u\right)_{1:(m-1)K_t \times N_m}$
  $\bar{\mathbf{H}}_u^{m,2} = \left(\mathbf{H}_u\right)_{mK_t+1:K \times N_m}$
  $\bar{\mathbf{H}}_f^{m,1} = \left(\mathbf{H}_f\right)_{1:(m-1)N_t \times N_m}$
  $\bar{\mathbf{H}}_f^{m,2} = \left(\mathbf{H}_f\right)_{mN_t+1:N \times N_m}$
  repeat;

The design of $\mathbf{T}_{a_m}$ can be established by the concept of null space projection in linear algebra. In fact, we use the null space of $\bar{\mathbf{H}}_f^m$ to be ensure that

$$\bar{\mathbf{H}}_f^m \mathbf{T}_{a_m} = \mathbf{0} \tag{22}$$

Unfortunately, as noted earlier, $\bar{N}_m > N_m$, so that the null space of matrix $\bar{\mathbf{H}}_f^m$ is empty. To cope with this problem, we resort to a regularized version of matrix $\bar{\mathbf{H}}_f^m$:

$$\mathbf{H}_f^{reg,m} = \mathbf{H}_f^t \mathbf{H}_f^{t,H} + \mathbf{I}_N \tag{23}$$

$$\mathbf{H}_f^t = \begin{pmatrix} \mathbf{H}_f^m \\ \bar{\mathbf{H}}_f^m \end{pmatrix} \tag{24}$$

where this regularized version of a matrix was previously applied for terrestrial networks in [12].
Now, $\mathbf{H}_f^{reg,m}$ is of size $N \times N$. Let us construct $\bar{\mathbf{H}}_m^{reg,m}$ (which denotes the regularized version of $\bar{\mathbf{H}}_f^m$) by selecting last $(N - N_m)$ rows of matrix $\bar{\mathbf{H}}_f^{reg,m}$ so that the singular decomposition entails

$$\bar{\mathbf{H}}_f^{reg,m} = \bar{\mathbf{U}}_f^{reg,m} \bar{\mathbf{\Sigma}}_f^{reg,m} (\bar{\mathbf{V}}_f^{reg,m} \bar{\mathbf{V}}_f^{0,m})^H \tag{25}$$

where $\bar{\mathbf{V}}_f^{0,m}$ represents the null space of matrix $\bar{\mathbf{H}}_m^{eq,m}$. Then, the design of $\mathbf{T}_{a_m}$ can be expressed as

$$\mathbf{T}_{a_m} = \bar{\mathbf{V}}_f^{0,m}. \tag{26}$$

Once the feeder link interference is accounted for, the second-stage precoder design is completed by addressing the inter and intra-cluster interference parameterized by $\mathbf{H}_u$. The corresponding M-ZF and M-MMSE precoders for the m-th gateway are written as follows [6]:

$$\mathbf{T}_{b,m}^{\text{ZF}} = \sqrt{\alpha_m} \hat{\mathbf{V}}_u^{0,m} (\hat{\mathbf{V}}_u^{0,m})^H \mathbf{H}_u^{m,H} (\mathbf{H}_u^m \hat{\mathbf{V}}_u^{0,m} (\hat{\mathbf{V}}_u^{0,m})^H \mathbf{H}_u^{m,H})^{-1}, \tag{27}$$

$$\mathbf{T}_{b,m}^{\text{MMSE}} = \sqrt{\alpha_m} \hat{\mathbf{V}}_u^{0,m} (\hat{\mathbf{V}}_u^{0,m})^H \mathbf{H}_u^{m,H} (\mathbf{H}_u^m \hat{\mathbf{V}}_u^{0,m} (\hat{\mathbf{V}}_u^{0,m})^H \mathbf{H}_u^{m,H} + \mathbf{I}_{N_m})^{-1}. \tag{28}$$

The parameter α_m is such that

$$\text{trace}\big(\mathbf{H}_f^m \mathbf{T}_m \mathbf{T}_m^H \mathbf{H}_f^{m,H}\big) \leq P_m \tag{29}$$

with P_m denotes the total transmit power by N_m feeds. Note that, similarly to the feeder link channel, we can use the null space of matrix $\bar{\mathbf{H}}_u^m$ to avoid intra and inter-cluster interference at m-th gateway and guarantee $\bar{\mathbf{H}}_u^m \mathbf{T}_m = \mathbf{0}$. keeping in mind that $\bar{\mathbf{H}}_u^m$ is of size $\bar{K}_m \times N_m$, obtaining the null space of $\bar{\mathbf{H}}_u^m$ depends on the different values of N_m and $\bar{K}_m$:

- $\bar{K}_m < N_m$, employing Singular Value Decomposition (SVD) on $\bar{\mathbf{H}}_u^m$ leads to

$$\bar{\mathbf{H}}_u^m = \hat{\mathbf{U}}_u^m \hat{\mathbf{\Sigma}}_u^m (\hat{\mathbf{V}}_u^m \hat{\mathbf{V}}_u^{0,m})^H \tag{30}$$

  where $\hat{\mathbf{V}}_u^{0,m}$ denotes the null space of matrix $\bar{\mathbf{H}}_u^m$.
- $\bar{K}_m > N_m$, the null space of matrix $\bar{\mathbf{H}}_u^m$ is empty. The solution to find the null space of matrix $\bar{\mathbf{H}}_u^m$ is resemble to the $\bar{\mathbf{H}}_f^m$ in (23).

Not only this is interesting but also this is important to point out that in order to reject inter-cluster and inter-feeder links interference, the $\mathbf{T}_m$ requires perfect CSI from other gateways, leading to large system resources overhead. In contrast to previous works, this paper proposed the case where a two-stage precoding scheme alleviates the exchange of CSI among the gateways with respect to a one-shot precoding computation. In fact, for the two-stage case m-th gateway needs to obtain CSI of sub-matrices $\bar{\mathbf{H}}_u^m$ and $\bar{\mathbf{H}}_f^m$ of channel matrices $\mathbf{H}_u$ and $\mathbf{H}_f$. However, designing one-stage precoding implies each gateway must obtain the global channel matrix combination $\mathbf{H} = \mathbf{H}_u \mathbf{H}_f$.

As expected, accounting for the feeder link non-ideality can only degrade the performance with respect to the conventional transparent feeder link assumption. A formal proof is provided in the Appendix A.

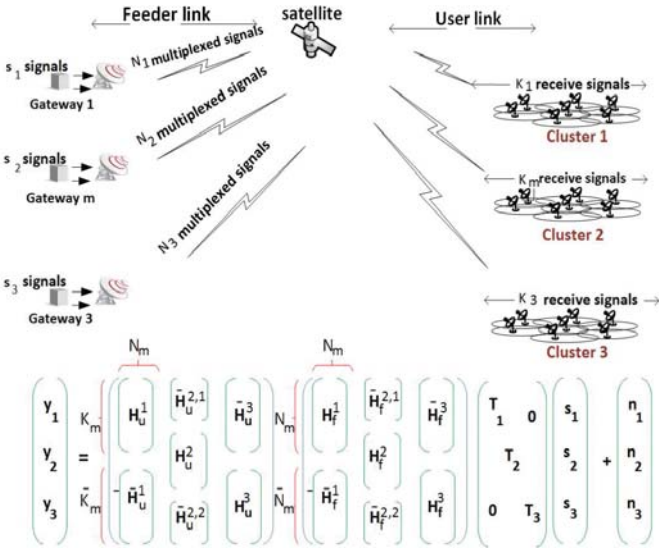

Fig. 2: Multiple gateway system architecture and block diagram of three gateway and clusters.

IV. Numerical Results

In order to further compare the performance of the proposed scenarios in this study, Monte Carlo simulations have been carried out. The simulation setup is based on an array fed reflector antenna which has been provided by ESA in the framework of SatNEx III project. In this context, the number of feeds is assumed to be $N = 155$ and $K = 100$ beams are covering the whole Europe area. The feeder link signal streams are the same as the on-board feed signals at the satellite.
Results have been averaged for a total of 500 user link channel realizations, for a user link total available bandwidth of 500 MHz (in Ka band). Moreover, the bandwidth is divided into M = 12 carriers. Still, the results will be presented for the total bandwidth (i.e. by summing the contribution of each carrier) and as a function of the total power denoted by P_T which accounts for the transmit power of all carriers, that is $P_T = MP$. P denotes the power budget that is distributed among the transmit beams. The rest of simulation parameters are indicated in Table I. As channel impairments, only atmospheric fading, with statistics corresponding to the city of Amsterdam, is considered.

For the sake of illustration, we assume the following simple inter-feeder link interference model for matrix $\mathbf{H}_f$:

$$[\mathbf{H}_f]^{i,i} = \mathbf{I}_{N_t}, \tag{31}$$

$$[\mathbf{H}_f]^{i,j} = \rho^{|i-j|} \mathbf{E}_{N_t} \quad i \neq j, \tag{32}$$

for $i = 1, \ldots, F$ and $j = 1, \ldots, F$. The parameter $\rho \in [0, 1]$ quantifies the amount of interference as a decreasing function of the gateway index difference.

As performance metrics, the SINR per user was computed, and then the corresponding spectral efficiency was obtained from the DVB-S2x standard [14]. The simulation results include also the availability based on the cumulative distribution

TABLE I: USER LINK SIMULATION PARAMETERS

Parameter	Value
Satellite height	35786 km (geostationary)
Satellite longitude, latitude	$10° East, 0°$
Earth radius	6378.137 Km
Feed radiation pattern	Ref: [13]
Number of feeds N	155
Number of beams	100
User location distribution	Uniformly distributed
Carrier frequency	20 GHz (Ka band)
Total bandwidth	500 MHz
Number of carriers M	12
Atmospheric fading	Rain fading
Roll-off factor	0.25
User antenna gain	41.7 dBi
Multibeam satellite antenna gain	Ref: [13]

function (CDF) of the SINR. In this case, the instantaneous availability indicator for the k-th user is given by

$$A_k = g(\gamma_k) \tag{33}$$

which is equal to 0 if the user is unavailable, i.e., if its instantaneous SINR is lower than that required by the lowest ModCod of DVB-S2x, $\gamma_k < -2.85$dB, and is equal to 1 otherwise.

As upper bound reference scenario a multiple gateway architecture is chosen with a transparent feeder-link. Full frequency reuse in this reference scenario is addressed by M-ZF precoding at each gateway so that the signal model is expressed in (2), considering $\mathbf{H}_f = \mathbf{I}_N$. In this context, the precoding technique in (21) for m-th gateway (respectively for all gateways with $m = 1, ..., F$) can be rewritten as

$$\mathbf{T}_m = \mathbf{T}_{b_m} \quad m = 1, \ldots, F \tag{34}$$

where $\mathbf{T}_{b_m}$ is expressed in (27) so that $\mathbf{T}_{a_m} = \mathbf{I}_{N_m}$ would be sufficient.

As lower bound scenario, the m-th gateway employs a conventional ZF precoder which is only able to cope with intra-cluster interference:

$$\mathbf{T}_m = \mathbf{T}_{b_m} = \sqrt{\alpha_m}\mathbf{H}_u^m(\mathbf{H}_u^m\mathbf{H}_u^{m,H})^{-1} \quad m = 1, \ldots, F. \tag{35}$$

Thus, interference parameterized by $\bar{\mathbf{H}}_f^m$ and $\bar{\mathbf{H}}_u^m$, both inter-feeder link and inter-cluster interferences, respectively, are not considered for the precoding design. For the simulations $F = 14$ gateways/clusters were considered, with each cluster containing seven or eight beams. Note that the analysis in Section III assumed an identical number of beams per cluster; in practice, this can be easily extended to heterogeneous configurations as the one provided by ESA. The performance of both M-ZF and M-MMSE precoders characterized by Equations (26-28) is illustrated in Figures 3 and 4. Figure 3 (left) depicts the total throughput of the satellite. As illustrated, the proposed precoding schemes provide a significant gain with respect to the conventional ZF scheme (i.e, lower bound scenario) in (35). This is due to the enhanced capability to cope with the inter/intra user cluster and inter-feeder link interference at each gateway. For this figure, the amount of feeder link interference corresponds to $\rho = 1$ in (32). The improvement can be also noticed from the corresponding availability plots in Figure 3 (right) with the throughput gain matching the availability improvement. It is easily seen that the availability of the system with new proposed design of M-ZF and M-MMSE precoders is much closer to the upper-bound scenario than the lower-bound reference and this is due to a significant reduction of inter/intra user cluster and inter-feeder link interference at each gateway.

Figure 4 compares the results of the proposed precoding schemes considering that each gateway receives interference from 1 to 5 gateways. The transmit power is set to $P_T = 30dBW$. Evidently, even with only one interfering gateway, the average spectral efficiency significantly decreases with respect to the ideal feeder-link scenario. Nevertheless, a significant improvement comes from the use of M-ZF and M-MMSE at the gateways to fight the feeder link interference.

For the sake of completeness, Figure 4 also shows the performance of our proposals for different values of ρ. It is justified that a large amount of variation ρ in the feeder links leads to a significant degradation of the system performance. In other words, the higher ρ, the lower throughput (i.e. spectral efficiency) will be. Nevertheless, our proposed M-ZF and M-MMSE schemes provide a potential advantage in order to compensate throughput degradation through the impact of inter-feeder and intra/inter cluster interferences.

Consequently, employing multiple gateway dimension leads to drastically increase the available feeder link bandwidth resource. However, the inter-feeder link interference dimension limits the effectiveness of interference mitigation techniques and therefore the system throughput is decreased with respect to the level of interference in the user and feeder links at multiple gateway architecture.

More elaborate interference mitigation technique based on collaboration among gateways is left for future works.

V. CONCLUSION AND FUTURE WORK

In this paper, we have considered the problem of multiple gateway architecture in the forward link of multibeam satellites, with each gateway handling a set of beams. Under this context, we proposed novel M-ZF and M-MMSE precoding schemes for full frequency settings in both feeder and user links. As a result of the derived scheme, the impact of the inter-feeder link interference was reduced significantly after increasing the exchanged CSI information among the gateways.

Finally, the proposed multiple gateway architecture assumed that a single user per individual beam is served at each time instant. However, next generation multiple gateway multibeam satellite communications should be able to operate in a multicast fashion since data from different users is embedded in the same frame. Precisely, in order to increase the coding gain, each beam simultaneously serves more than one user by means of transmitting a single coded frame. This scheme entails a modification of the overall precoding design at each gateway since more than one spatial signature per beam must be considered. The extension of the presented results to this setting is a line of further research.

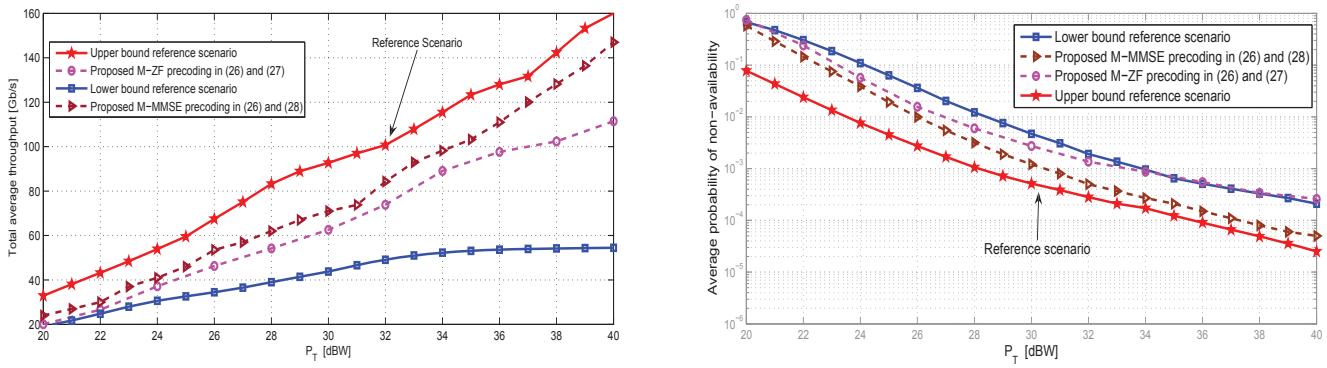

Fig. 3: Average throughput (Gb/s) comparison based on DVB-S2x MODCOD (left) and CDF of SINR comparison when the rain fading is considered (right). The interfering parameter over feeder link is $\rho = 1$. The number of gateways/clusters is 14.

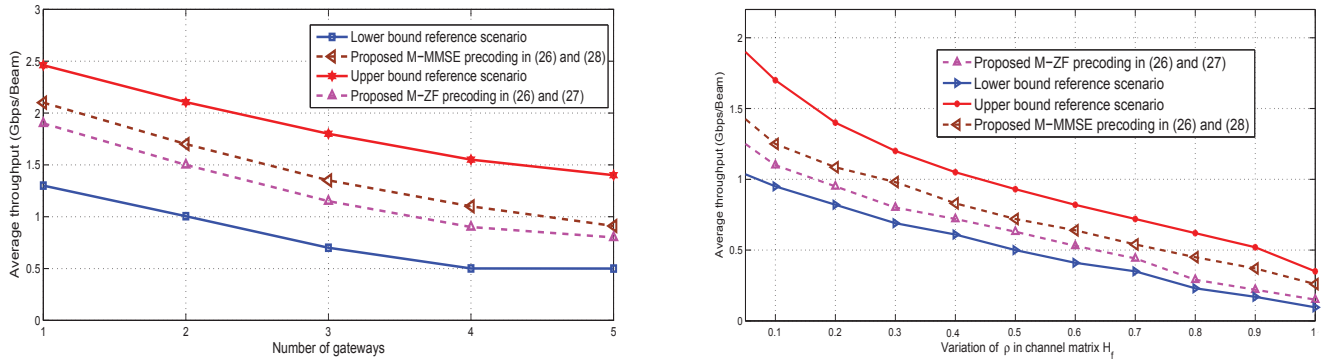

Fig. 4: Average throughput per beam versus number of gateways (left). The interfering parameter is set to 1 ($\rho = 1$). Average throughput per beam for different amounts of inter-feeder link interference ρ (right).

APPENDIX A

It is natural to think that considering impact of feeder and user link channels jointly can perform worse than considering user link effect. This statement is analytically proved in this Appendix.

Let us consider ZF precoding to equalize Signal to Noise Ratio (SNR) among K users. Then, the resulting SNR, computed from (11) and (14), can be written as

$$\text{SNR} = \frac{P}{\text{trace}(\mathbf{H}_f(\mathbf{H}_f^H\mathbf{H}_u^H\mathbf{H}_u\mathbf{H}_f)^{-1}\mathbf{H}_f^H)} \tag{36}$$

where the m subscript has been omitted for the sake of clarity. Conventionally, a noiseless and perfectly calibrated feeder link implies:

$$\mathbf{H}_f = \mathbf{I}_N. \tag{37}$$

Then, the signal model in (2) can be rewritten as

$$\mathbf{y} = \mathbf{H}_u\mathbf{x} + \mathbf{n} \tag{38}$$

and the precoding matrix in (11) can also be expressed as

$$\mathbf{T} = \sqrt{\alpha}\mathbf{H}_u^H\left(\mathbf{H}_u\mathbf{H}_u^H\right)^{-1}. \tag{39}$$

which yields the following SNR in the coverage area:

$$\text{SNR}_{non} = \frac{P}{\text{trace}(\mathbf{H}_u\mathbf{H}_u^H)^{-1}} \tag{40}$$

Prior to establishing the relation between the SNR of these two cases, the following lemma is introduced.

Lemma 1. *The* $\mathbf{U}$ *and* $\mathbf{V}$ *are* $n \times n$ *matrices, then*

$$\sum_i \lambda_i(\mathbf{UV}) \geq \sum_i \lambda_i(\mathbf{U})\lambda_{n-i+1}(\mathbf{V}) \quad i = 1, \ldots, n. \tag{41}$$

Proof, [12].

With this result, the following theorem can be established.

Theorem 1. *For any semi-definite positive matrix* $\mathbf{H}_f$*, it results that*

$$SNR_{non} \geq SNR \tag{42}$$

Proof. See Appendix B.

Therefore, the system experiences a larger interference since the effect of interference among gateways on the feeder link is taken into account.

APPENDIX B

The following inequality $\text{SNR} \geq \text{SNR}_{non}$ entails that

$$\text{trace}(\mathbf{H}_f(\mathbf{H}_f^H\mathbf{H}_u^H\mathbf{H}_u\mathbf{H}_f)^{-1}\mathbf{H}_f^H) \leq \text{trace}(\mathbf{H}_u\mathbf{H}_u^H)^{-1} \tag{43}$$

First, with the following SVD of the channel matrix $\mathbf{H}_u = \mathbf{U}_u\mathbf{\Phi}_u\mathbf{V}_u^H$, let us simplify the left-hand side of (43) as follows

$$\text{trace}(\mathbf{H}_u\mathbf{H}_u^H)^{-1} = \sum_k \frac{1}{\lambda_k(\mathbf{H}_u\mathbf{H}_u^H)} = \sum_k \frac{1}{\lambda_k(\mathbf{\Phi}_u\mathbf{\Phi}_u^H)} \tag{44}$$

where $\lambda_k(.)$ denotes the k-th largest singular value of respective matrix.
Similarly, with $\mathbf{H}_f = \mathbf{M}_f\mathbf{\Sigma}_f\mathbf{L}_f^H$, the right-hand side in (43) can be worked out as

$$\text{trace}(\mathbf{H}_f(\mathbf{H}_f^H\mathbf{H}_u^H\mathbf{H}_u\mathbf{H}_f)^{-1}\mathbf{H}_f^H) = \text{trace}[(\mathbf{A}^H\mathbf{A})^{-1}(\mathbf{\Phi}_u\mathbf{\Phi}_u^H)^{-1}] \tag{45}$$

where $\mathbf{A}$ is defined as follows

$$\mathbf{A} \triangleq \mathbf{V}_u^H\mathbf{M}_f = \begin{pmatrix} \mathbf{A}_1 & \mathbf{A}_2 \\ \mathbf{A}_3 & \mathbf{A}_4 \end{pmatrix} \tag{46}$$

with the submatrix $\mathbf{A}_1$ is of size $K \times K$. Moreover, $\mathbf{A}_2$ and $\mathbf{A}_3^H$ both are submatrices of size $K \times (N-K)$, and submatrix $\mathbf{A}_4$ is of size $(N-K) \times (N-k)$.
Now, we have to prove that

$$\begin{aligned} \lambda_k(\mathbf{A}_1^H\mathbf{A}_1) \leq 1, \qquad \forall k, \\ \lambda_k(\mathbf{A}_4^H\mathbf{A}_4) \leq 1, \qquad \forall k. \end{aligned} \tag{47}$$

In fact, $\mathbf{A}$ is a unitary matrix which holds

$$\mathbf{A}_1^H\mathbf{A}_1 + \mathbf{A}_3^H\mathbf{A}_3 = \mathbf{I}. \tag{48}$$

$$\mathbf{A}_2^H\mathbf{A}_2 + \mathbf{A}_4^H\mathbf{A}_4 = \mathbf{I}. \tag{49}$$

with the following eigenvalue decompositions $\mathbf{A}_1^H\mathbf{A}_1 = \mathbf{S}_1\mathbf{\Psi}_1\mathbf{S}_1^H$ and $\mathbf{A}_4^H\mathbf{A}_4 = \mathbf{S}_4\mathbf{\Psi}_4\mathbf{S}_4^H$, (48) can be rewritten as

$$\mathbf{\Psi}_1 = \mathbf{S}_1^H\mathbf{I}\mathbf{S}_1 - \mathbf{S}_1^H\mathbf{A}_3^H\mathbf{A}_3\mathbf{S}_1 \tag{50}$$

$$\mathbf{\Psi}_4 = \mathbf{S}_4^H\mathbf{I}\mathbf{S}_4 - \mathbf{S}_4^H\mathbf{A}_2^H\mathbf{A}_2\mathbf{S}_4 \tag{51}$$

where $\mathbf{\Psi}_1 = \text{diag}\big(\lambda_1(\mathbf{A}_1^H\mathbf{A}_1), ..., \lambda_K(\mathbf{A}_1^H\mathbf{A}_1)\big)$ and $\mathbf{\Psi}_4 = \text{diag}\big(\lambda_1(\mathbf{A}_4^H\mathbf{A}_4), ..., \lambda_{(K-N)}(\mathbf{A}_4^H\mathbf{A}_4)\big)$.
It is clear that both $\mathbf{S}^H\mathbf{A}_3^H\mathbf{A}_3\mathbf{S}$ and $\mathbf{S}^H\mathbf{A}_2^H\mathbf{A}_2\mathbf{S}$ have to be diagonal. Moreover, since $\mathbf{S}^H\mathbf{A}_2^H\mathbf{A}_2\mathbf{S}$ and $\mathbf{A}_3^H\mathbf{A}_3$ are semi positive definite, it has to have positive elements on the diagonal which proves (47). Eventually, employing Lemma 1 leads to

$$\begin{aligned} &\text{trace}[(\mathbf{A}^H\mathbf{A})^{-1}(\mathbf{\Phi}_u\mathbf{\Phi}_u^H)] \geq \\ &\sum_k \frac{1}{\lambda_{K-k+1}(\mathbf{A}^H\mathbf{A})}\frac{1}{\lambda_k(\mathbf{\Phi}_u\mathbf{\Phi}_u^H)} \geq \sum_k \frac{1}{\lambda_k(\mathbf{\Phi}_u\mathbf{\Phi}_u^H)} \end{aligned} \tag{52}$$

and concludes the proof.

REFERENCES

[1] G. Maral and M. Bousquet, *"Satellite communications systems: systems, techniques and technology,"* 5th edition, wiley Press, ISBN: 978-0-470-71458-4 , December 2009.

[2] G. Gallinaro, M. Debbah, G. Gallinaro, R. Mueller, M. Neri and R. Rinaldo *"Novel intra-system interference mitigation techniques and technologies for next generations broadband satellite systems,"* Final report of ESA/ESTEC contract No. 18070/04/NL/US, 2008.

[3] L. Cottatellucci, M. Debbah, G. Gallinaro, R. Mueller, M. Neri and R. Rinaldo *"Interference mitigation techniques for broadband satellite systems,"* 24th AIAA International Communications Satellite Systems Conference (ICSSC), pp. 1-12, June 2006.

[4] V. Joroughi, B. Devillers, M. Vaźquez and A. Ana Perez-Neira, *"Design of an on-board beam generation process for the forward link of a multi-beam broadband satellite system,"* IEEE Global Telecommunications Conference (GLOBECOM), pp. 1-7, December 2013.

[5] A. Gharanjik, B. Mysore Rama Rao, P. Arapoglou, and B. Ottersten, *"Multiple gateway transmit diversity in Q/V band feeder links,"* IEEE Transactions on Communications, vol. 99, pp. 1-12, January 2014.

[6] V. Joroughi, M. A. Vaźquez and A. Perez-Neira, *"Multiple gateway precoding with per feed power constraints for multibeam satellite systems,"* 20th European Wireless Conference (EW-14), pp. 1-7, May 2014.

[7] G. Zheng, S. Chatzinotas and B. Ottersten, *"Gateway cooperation in multibeam satellite systems,"* 23rd IEEE International Symposium on Personal Indoor and Mobile Radio Communications (PIMRC), pp. 1-6, September 2012.

[8] ITU-R Recommendation P.618-10, *"Propagation data and prediction methods required for the design of Earth-space telecommunication systems,"* Geneva 2009.

[9] J. Arnau, B. Devillers, C. Mosquera and A. Pérez-Neira, *"Performance study of multiuser interference mitigation schemes for hybrid broadband multibeam satellite architectures,"* EURASIP Journal on Wireless Communications and Networking, no. 1, p. 132, February 2012. [Online]. Available: http://jwcn.eurasipjournals.com/content/2012/1/132

[10] SM Kay,*"Fundamentals of statistical signal processing: estimation theory,"*Prentice-Hall, Inc. Upper Saddle River, NJ, USA, 1993.

[11] AW. Marshall and I. Olkin,*"Inequalities: Theory Of Majorization and its Applications,"* Academic Press, NewYork, NY, 1979.

[12] Y. Silva and A. Klein, *"Linear transmit beamforming techniques for the multigroup multicast scenario,"* IEEE Transactions on Vehicular Technology, vol. 58, no. 8, pp. 43534367, October 2009.

[13] Call of Order 2-Task 1, *"Fair comparison and combination of advanced interference mitigation techniques,"* Satellite Network of Experts (SatNEx) 3, report of ESA contract NO:23089/10/NL/CPL.

[14] ETSI EN 302 307-2: *"Digital Video Broadcasting (DVB); Second generation framing structure, channel coding and modulation systems for Broadcasting, Interactive Services, News Gathering and other broadband satellite applications; Part 2: DVB-S2 Extensions (DVB-S2X)."*